CDCC-07

DURABILITY AND FIELD APPLICATIONS OF FIBRE REINFORCED POLYMER (FRP) COMPOSITES FOR CONSTRUCTION

DURABILITÉ ET APPLICATIONS DES COMPOSITES EN POLYMÈRES RENFORCÉS DE FIBRES (PRF) POUR LA CONSTRUCTION

ULTIMATE AND SERVICE BEHAVIOUR OF GFRP RC BRIDGE DECK SLABS SUBJECTED TO FATIGUE LOADING

A. El-Ragaby [1], E. F. El-Salakawy [2] and B. Benmokrane [3]

[1] PhD Candidate, Dept. of Civil Engineering, University of Sherbrooke, Canada
[2] CRC Professor, Dept. of Civil Engineering, University of Manitoba, Winnipeg, Canada
[3] NSERC Chair Professor, Dept. of Civil Engineering, University of Sherbrooke, Canada

ABSTRACT

The accumulated fatigue damage due to the increase in traffic loads and volume as well as the corrosion of the internal steel reinforcement have resulted in severe deterioration of concrete bridge deck slabs. Recently, glass fibre-reinforced polymer composites (GFRP) have been widely used as internal reinforcement for concrete bridge deck slabs to over come the corrosion related problems. However, the performance of FRP-reinforced concrete elements subjected to cyclic fatigue loading, which is a critical design limit for bridge decks, has not been fully explored. Therefore, this research was designed to investigate the service and ultimate behaviour of concrete bridge deck slabs reinforced with GFRP bars under fatigue loading. A total of five full-scale deck slab prototypes were subjected to fatigue loading and then tested under concentrated monotonic loading till failure. Different ratios and configurations of GFRP reinforcement were used. Also, different schemes of accelerated fatigue loading representing service loading condition and lifetime equivalent traffic loading were used. All the test prototypes were subjected to actual environmental conditions for more than one year before testing. The test results showed the superior fatigue performance and high residual static capacity of concrete bridge deck slabs reinforced with glass FRP composite bars compared to steel.

1. INTRODUCTION

The North American infrastructures have been adversely affected by age and weathering over the past two decades. In particular, highway concrete bridges suffer from premature structural decay as a result of steel reinforcement corrosion. Because the rehabilitation cost of a corroded infrastructure has become so enormous, FRP composites are gaining increased acceptance to be used in bridge applications, due to their non-corrodible nature. FRP also possesses several properties such as high strength, lightweight and consequent ease of field placement, which make it a suitable alternate to conventional steel reinforcement in RC bridge decks [1].

On the other hand, deterioration of concrete bridge deck slabs is not due to the corrosion effects only. During the last two decades, more researchers and transportation agencies began to recognize that truck wheel load is also an important factor in deteriorating RC bridge decks. In general, fatigue is an important limit state that must be considered by designers of bridges where the bridge deck must be designed to ensure adequate safety and durability during the design life under both static and fatigue considerations [2]. It is well documented now that bridge deck slabs resist the traffic loads by arching action and always fail in punching shear [3, 4]. When using FRP bars as internal reinforcement for RC elements, and due to the relatively low modulus of elasticity and small transverse strength of FRP bars, the overall shear capacity of concrete members reinforced with FRP bars as flexural reinforcement is lower than that of concrete members reinforced with the same amount of steel [5-7]. Moreover, the shear strength of RC members degrades faster with cycling loading than their flexural strength. This is mainly because of the gradual reduction of aggregate interlock along cracks, as their interfaces are ground and become smoother and wider with cycling. Consequently, the proportioning of members of new RC structures in shear and the evaluation of members of existing substandard structures should take into account the reduction of shear resistance due to cyclic loading below the value applying for monotonic loading [8].

In the available literature, little research has been carried out to investigate the behaviour of concrete bridge deck slabs reinforced with FRP bars under monotonic loading conditions. However, experimental data regarding their performance and durability under fatigue loads are still lacking. As the behaviour of FRP reinforced concrete elements cannot be extrapolated from that of the steel reinforced ones, more research studies and investigations on such elements are needed. Therefore, this research is designed to investigate the performance of concrete bridge deck slabs reinforced with glass FRP reinforcing bars under the effect of wheel cyclic (fatigue) and monotonic loads. The current research includes experimental testing of full-size GFRP RC deck slab prototypes carried out in two phases. The first experimental phase investigated the behaviour under fatigue loading till failure. The second phase of the experimental program investigated the behaviour of the test prototypes subjected to certain number of cyclic loading then loaded monotonically to failure. This paper is focusing on the test procedure and results of the second experimental phase. A brief summary about the test results of the first phase is presented in the following sections.

2. THE EXPERIMENTAL PROGRAM

2.1 Test Prototypes

The experimental program included casting and testing of nine full-size bridge deck slab prototypes (2500 mm width, 3000 mm length, and 200 mm thick). The slabs were tested on two phases. Phase I included four deck slabs. Three slabs S1, S3, and S4 were reinforced with GFRP bars. The three slabs have identical bottom reinforcement (1.2% and 0.6% in the transverse and longitudinal direction, respectively). For the top reinforcement layer, a reinforcement ratio of 0.6% and 0.3% for slabs S1 and S3, respectively, was used in both directions. Slab S4 had no top reinforcement. The fourth slab, S0, was reinforced with steel bars (0.3% top and bottom in both directions) for comparisons. Phase II included five deck

slabs; S2, S3-C, S4-C, S5-C and S6-C, entirely reinforced with GFRP bars. The five deck slabs were divided into three different test groups according to the reinforcement ratios and configurations or the type of fatigue loading. Group *I* contained one slab prototype, S2, which was reinforced identically as slab S1 in phase I. The bottom transverse GFRP reinforcement was calculated based on the empirical design method recommended by the second edition of Canadian Highway Bridge Design Code, CHBDC [9]; Clause 16.8.7.1. According to this clause, a minimum FRP reinforcement area in the transverse bottom direction is set to $500d_s/E_{frp}$ where d_s is the distance from the top of the slab to the centroid of the bottom transverse reinforcement. This approach resulted in using No.19 GFRP bars spaced at150 mm in the bottom transverse direction with a reinforcement ratio of 1.2%. The longitudinal bottom reinforcement and the top reinforcement in both directions consisted of No.16 GFRP bars spaced at 200 mm providing a reinforcement ratio of 0.6%.

Group II contained two test prototypes, S3-C and S4-C, which were reinforced identically as slabs S3 and S4 in phase I. They have the same bottom reinforcement as S2. For the top reinforcement layers, different configurations and reinforcement ratios were used. For slab S3-C a minimum reinforcement ratio of 0.35% (according to CHBDC) was used in both directions, which results in using No.13 GFRP bars spaced at 300 mm in each direction. For slab S4-C, no top reinforcement was used. Group III included two test prototypes, designated as S5-C and S6-C. The bending moments in these deck slabs were calculated according to the flexural design method (general approach – Clauses 5.4, 5.5, 5.6, 5.7, 8.8, 8.9, 8.12, and 8.13) specified in the CHBDC [9]. A new approach was used in the design of the GFRP reinforced deck slab. This approach, which has been recently proposed by the Ministry of Transportation of Quebec (MTQ), uses the calculated bending moments to select the required FRP reinforcement ratio based on satisfying a specific maximum crack width and stress limits, rather than transformation of steel reinforcement to FRP bars based on stiffness and strength equivalences. A maximum crack width of 0.5 mm and stress limits of 30% and 15% of the GFRP ultimate tensile strength under service and sustained loads, respectively, were used. Since the calculations of the crack width depend on the bond coefficient, k_b, using two different values of k_b results in two different reinforcement ratios. A value of k_b equals 1.2 and 0.8 was used for slabs S5-C and S6-C, respectively. Table 1 summarizes the reinforcement details of the five deck slab prototypes of phase II.

Table 1: Reinforcement details of test prototypes

Slab	Transverse Direction		Longitudinal Direction	
	Bottom	Top	Bottom	Top
S2	No.19 @150 mm ρ =1.20 %	No.16 @ 200 mm ρ =0.60 %	No.16 @ 200 mm ρ =0.60 %	No.16 @ 200 mm ρ =0.60 %
S3-C	No.19 @150 mm ρ =1.20 %	No.13 @ 300 mm ρ =0.35 %	No.16 @ 200 mm ρ =0.60 %	No.13 @ 300 mm ρ=0.35 %
S4-C	No.19 @150 mm ρ =1.20 %	No Reinforcement	No.16 @ 200 mm ρ =0.60 %	No Reinforcement
S5--C	No.19 @100 mm ρ =1.80 %	No.19 @75 mm ρ =2.80 %	No.16 @150 mm ρ =1.00 %	No.16 @150 mm ρ =1.00 %
S6-C	No.19 @140 mm ρ =1.40 %	No.19 @140 mm ρ =1.40 %	No.16 @200 mm ρ =0.60 %	No.16 @200 mm ρ =0.60 %

2.2 Test Set-up

The test prototypes were supported longitudinally on two steel girders (built up I-beam section) spaced at 2000 mm center-to-center which were connected together with three cross frames to prevent the lateral movement. To account for the continuity effect in a real bridge, the deck slabs were partially restraint against rotations and lateral displacements. More details about the test set-up can be found elsewhere [10, 11]. All the deck slab test prototypes were tested under a single concentrated load at the center of a clear span of 2000 mm. Figure 1 shows a photo for the test set-up.

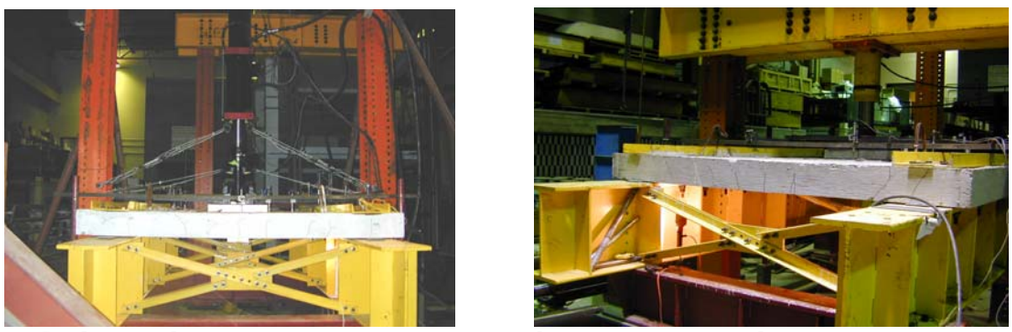

a- Cyclic Loading b- Monotonic Loading.

Fig. 1: The test set-up.

2.3 Loading Conditions

In this study, moving vehicular loads were simulated by stationary concentrated load varying cyclically in magnitude. Two schemes of fatigue loading were used, service conditions fatigue loading (used in Phase I) and equivalent life-time loading fatigue loading (used in Phase II).

Phase I investigated the behaviour under extremely high fatigue loading till failure. This phase was designed to evaluate the fatigue life and failure mode of such elements under fatigue loads. In this phase, an accelerated fatigue loading scheme was used. It consists of variable amplitude fatigue loading where all the slabs were subjected to sinusoidal waveform fatigue load cycles between a minimum load level (maintained at 15 kN) and variable peak load levels. Different peak loads of 183.8, 245.0, 367.5, and 490.0 kN were used. Each of the different fatigue loading steps (for example, between 15 kN and 183.75 kN peak load) was applied for 100,000 cycles at frequency of 2 Hz (Fig. 2). This fatigue loading scheme was applied to four deck slab prototypes (Slabs S1, S3, S4, and S0).

During Phase II, the cyclic loading scheme was designed, based on the findings of the first phase, to be equivalent to the lifetime loading that a real bridge may undergo. For deck slab S2, the fatigue loading scheme consisted of cyclic loading peaking at the service fatigue load level, which represents the service loading conditions. This loading scheme consisted of 4,000,000 load cycles of constant amplitude loading between a minimum load of 15 kN and a peak load of 122.5 kN (corresponding to P_{fls} according to CHBDC). It was applied at a frequency rate of 4 Hz (duration of about 12 days). This fatigue loading scheme

represents about twice the fatigue life recommended by other researchers and some design codes for bridge deck slabs [12].

Based on an analytical study conducted by the authors [10], it was possible to convert all the traffic volume and loads that a real bridge may experience during its expected service life to an accelerated fatigue loading at constant amplitude that is expected to produce the same damage. Having statistical data on the traffic volumes and loads on bridges available, 200,000 load cycles peaked at constant peak load of 245.0 kN (twice the fatigue service load, P_{fls}) was found to be equivalent, and even more, in damage to all the traffic volume and amplitudes on real bridge during 75 years service life. Consequently, four test prototypes, S3-C, S4-C, S5-C, and S6-C, were subjected to that fatigue loading scheme (duration of about 27.8 hours). The minimum load of 15 kN was kept unchanged.

All the deck slab prototypes were subjected to real environmental conditions (temperature fluctuation, freeze-thaw, and wet-dry cycles) for more than one year before tested (outdoor storage). Prior to applying the fatigue loading, all the test prototypes were pre-cracked by applying two monotonic load cycles (includes loading till 183.8 kN and unloading to zero). Similar monotonic load cycle was applied to the test prototypes after the fatigue loading conditions and before the final monotonic loading till failure. All the monotonic load cycles were applied in a displacement control mode at a rate of 0.8 mm/min. While, the final monotonic loading to failure was applied at a load-controlled rate of 5 kN/min using a manually-operated hydraulic jack.

3. SUMMARY OF THE RESULTS OF PHASE I

In Figure 3, it can be noticed that all the GFRP reinforced slabs had almost the same residual stiffness (fatigue damage) although they all have different reinforcement ratios in the top and bottom layers. It can be also noted that the magnitude of damage that was accumulated to the slab reinforced with steel was about 3 times greater than that of the GFRP reinforced ones. This reflected the superior performance of the GFRP-reinforced concrete bridge deck slabs under fatigue loading compared to the steel-reinforced ones. More details about the experimental testing and results of the first experimental phase and the analytical models can be found elsewhere [10, 11].

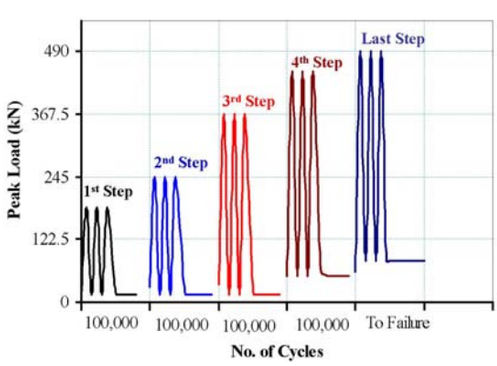

Fig. 2: Cyclic load Pattern (Phase I)

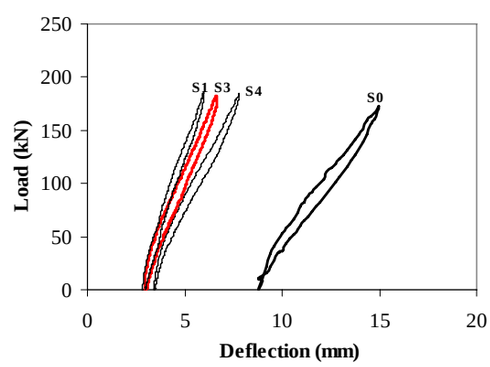

Fig. 3: Comparison between static responses of test prototypes after different fatigue loading steps

4. TEST RESULTS AND ANALYSIS OF PHASE II

4.1 Deflection Characteristics

Figure 4 shows the load-deflection behaviour of the five deck slab prototypes recorded during the initial two monotonic load cycles, which is referred to as ST-00 and ST-01 steps. It can be noticed that slabs S2, S3-C and S4-C had the same stiffness and load-deflection relationship (Fig. 4-a). Those three slabs have the same bottom reinforcement but with different top reinforcement ratios. The loading and unloading response was almost linear without a distinguished cracking point. The other two slabs, S5-C and S6-C showed a noticeable reduced stiffness and therefore larger deflections at the same load level. Slab S6-C had the same bottom reinforcement as slab S2, while slab S5-C had bottom transverse and longitudinal reinforcement 50% and 33%, respectively, more than those of slab S2. Also, both S5-C and S6-C had high reinforcement ratios in the top transverse layer of 2.8% and 1.2% in the transverse direction, respectively. Due to the significant difference in the transverse coefficient of thermal expansion between the GFRP bars and concrete, internal micro-cracks were expected in the concrete because of the environmental effects during the storage period. Although all the deck slab prototypes were subjected to the same environmental conditions, the internal concrete cracking status would become more sever when using higher reinforcement ratios. This, in turn, decreases the effective cross section and results in a reduced overall stiffness as noticed under mechanical loads in step ST-00. This might explain why those heavily reinforced deck slab prototypes had lower stiffness than the first three deck prototypes with low reinforcement ratios.

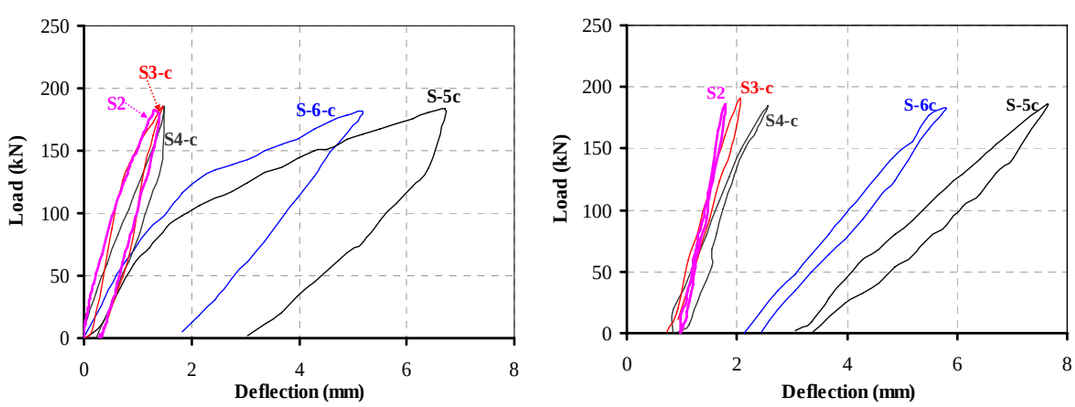

a- Initial, load cycle ST-00. b- Post-cracking, load cycle ST-01.

Fig. 4: Initial and post cracking load-deflection responses of test prototypes

The second monotonic load cycle, ST-01, was performed before applying any fatigue load cycles to asses the post cracking behaviour of the deck slab prototypes. As shown in Fig. 2-b, the post cracking responses of the five slab prototypes were linear with a reduced stiffness for slab prototypes with higher reinforcement ratio. Previous researches also indicated that the cracking status significantly affected the static and fatigue response of concrete deck slabs [13].

After being subjected to the cyclic fatigue loading, the test prototypes were subjected to a third monotonic load cycle, ST-02, similar to ST-01. The load cycle ST-02 aimed at assessing the fatigue damage and the degradation in the deck slabs after fatigue loading. From Figure 5-a, it can be noticed that slabs S3-C and S4-C had the same residual deflection and stiffness after being subjected to the same loading conditions. This indicated that they had the same fatigue damage, although S4-C had no top reinforcement at all. Also, slab S2 after being subjected to 4,000,000 load cycles at P_{fls} peak load had the lowest accumulated fatigue damage. Slabs S5-C and S6-C showed the largest residual deflections and lowest stiffness which indicated that they received the highest fatigue damage. This was mainly because of their higher content of reinforcement compared to the other tested slabs. As internal reinforcement represents points of discontinuity inside the concrete, higher reinforcement ratio results in more fatigue damage. This phenomenon was also noticed by other researchers who found that the fatigue life of the isotropic reinforced bridge decks was about 20 times that of the orthotropic reinforced ones under moving wheel-loads [14]. In addition, slabs S5-C and S6-C had higher reinforcement ratios than the other tested slabs S2, S3-C and S4-C particularly in the top reinforcement layer. This is also similar to previous observation for steel reinforced concrete decks where the fatigue life of the deck slabs with compressive reinforcement was found to be shorter than those without it [15].

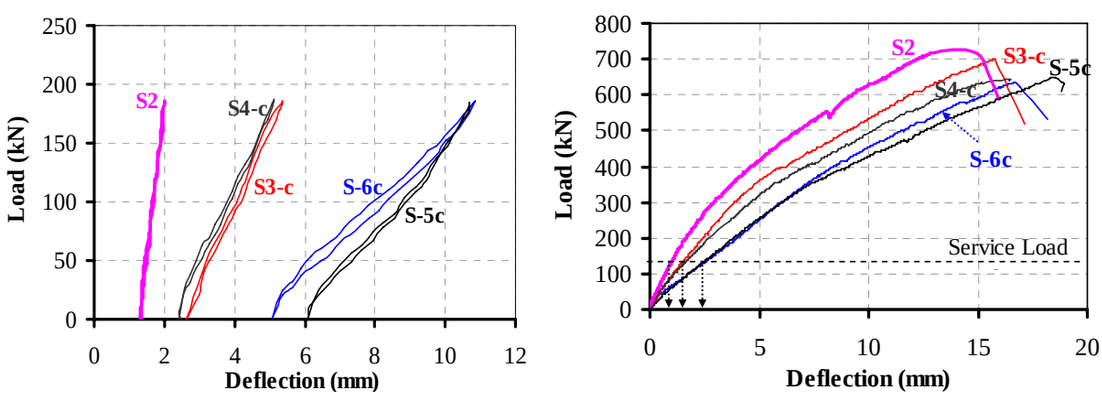

a- ST-02 monotonic load cycle. b- Final monotonic loading (till failure).

Fig. 5: Load-deflection responses after different loading conditions

Following the monotonic loading step ST-02, all the five deck slabs were loaded till failure under monotonic load. Figure 5-b presents comparisons of the load-deflection behaviour of the five slabs. Slabs S2 and S3-C had the highest residual ultimate capacity of about 719 and 700 kN respectively and the lowest deflection of about 15 mm. Slabs S4-C, S5-C and S6-C had approximately the same residual ultimate capacity of about 640 kN although they had different top and bottom reinforcement (even no top reinforcement for slab S4-C). As S5-C was the most affected deck slab by fatigue loading, it had the highest deflection of 19 mm compared to 17 mm for S6-C and S4-C. The higher deflection in S4-C compared to S3-C may be due to the deeper top longitudinal cracks over the supporting girders at higher loads in slab S4-C (without top reinforcement). However, all the deck slab prototypes showed deflection values less than 2.2 mm, at service load level, which is less than the

allowable limit recommended by AASTHO (L/800 = 2.5 mm) [16]. Finite element analyses on virgin test prototypes under monotonic loads only (no fatigue cyclic loads) showed that the maximum loss in the ultimate capacity of the deck slabs after being subjected to fatigue loads (which are expected to be more than the lifetime loading) did not exceed 15%. This loss in the ultimate capacity increased with the increase of internal reinforcement ratio, especially the top reinforcement ratio. Moreover, in terms of deflection, the ultimate deflections of the fatigued slabs were about 30% more than that of the virgin slabs which also reflected the deterioration in the deck stiffness. More details about the finite element analysis can be found elsewhere [17].

4.2 Failure Mode and Cracking Characteristics

All the bridge deck slab prototypes completed successfully the fatigue loading without failure. Then, they failed in punching shear mode under the final monotonic loading step. Figure 6 shows the failure shapes on the bottom surface of three different slabs. The final crack pattern had a flat fan shape. Slab S5-C, which had high bottom reinforcement ratio, had more cracks intensities (the cracks approximately have the same reinforcement spacing).

a- Slab S3-C b- Slab S4-C c- Slab S5-C

Fig. 6: Comparison of failure shapes and crack patterns on the bottom surface.

Figure 7 shows the cracks pattern at bottom surface of slab S5-C after fatigue loading compared to that at failure under monotonic load. It is clear that neither new cracks were developed nor existing cracks propagated under final monotonic loading. However, the existing cracks increased in width and penetration depth during the monotonic load.

a- After fatigue loading, slab S5-C b- After monotonic loading, slab S5-C

Fig. 7: Comparison of crack patterns on the bottom surface after different loading

5. CONCLUSIONS

A total of five full-size concrete deck slabs reinforced entirely with different reinforcement ratios and configurations of GFRP reinforcing bars were constructed. The deck slabs were subjected to different accelerated fatigue loading schemes represents either the service loading conditions or lifetime equivalent loading. Then, the test prototypes were loaded under concentrated monotonic loading till failure. Based on the experimental results, the following conclusions can be drawn:

1. During its service lifetime, a bridge deck slab is subjected to different number of wheel passes of different magnitudes. An accelerated, fixed amplitude fatigue loading equivalent in damage to lifetime traffic loading could be used to investigate the durability and residual strength of the bridge deck.
2. The glass FRP reinforced concrete bridge deck has a better fatigue performance and longer fatigue life (about 2.5 times) compared to the steel reinforced ones. This may be due to the close value of the modulus of elasticity for GFRP composite bars and concrete and the linear-elastic behaviour of GFRP bars up to failure.
3. GFRP-reinforced concrete bridge deck prototypes subjected to accelerated fatigue loading, causing equivalent damage to that of the lifetime service loading (peaking at the fatigue limit state load), have a residual ultimate static capacity of more than 85% of their ultimate capacity in virgin state (without any loading history).
4. The top reinforcement has a little effect on the performance of concrete bridge deck slab under fatigue loading peaking at the fatigue limit state load.
5. The maximum loss in the residual static capacity (equivalent to largest fatigue damage) was obtained for deck slabs that contained higher reinforcement ratio. This may be also attributed to the storage period of the prototypes.
6. The proposed FRP-reinforcement ratio adopted by the second edition of the CHBDC (CSA 2006) is adequate to meet the fatigue strength and fatigue life requirements of concrete bridge decks.

6. ACKNOWLEDGEMENTS

This research was financially supported by the National Science and Engineering Research Council (NSERC) of Canada, the Canadian Network of Centres of Excellence on Intelligent Sensing for Innovative Structures (ISIS Canada) and the Fonds québécois de la recherche sur la nature et les technologies (FQRNT).

7. REFERENCES

1. Benmokrane, B., El-Salakawy, E.F., Desgagné, G., and Lackey, T. "Building a New Generation of Concrete Bridge Decks using FRP Bars." Concrete International, the Magazine of ACI, 26 (8), 2004, pp. 84-90.
2. Youn, S.G. and Chang, S.P. ‘Behaviour of Composite Bridge Decks Subjected to Static and Fatigue Loading’ *ACI Journal Structural Journal*, 95 (3), 1998, 249-258.
3. Kuang, J.S., and Morley, C.T. ‘Punching Shear Behaviour of Restrained Reinforced Concrete Slabs’, *ACI Structural Journal*, 89 (1), 1992, 13-19.

4. Fang, I.K, Lee, J.H., and Chen, C.R. 'Behaviour of Partially Restrained Slabs under Concentrated Load', *ACI Structural Journal,* 91 (2), 1994, 133-139.
5. Hassan, T., Abdelrahman, A., Tadros, G., and Rizkalla, S. 'Fibre Reinforced Polymer Reinforcing Bars for Bridge Decks', *Canadian Journal of Civil Engineering,* 27, 2000, 839-849.
6. Ospina, C.E., Alexander, S.D.B., and Cheng, J.J.R. 'Punching of Two-Way Concrete Slabs with Fibre Reinforced Polymer Reinforcing Bars or Grids', *ACI Structural Journal,* 100 (5), 2003, 589-598.
7. Humar, J. and Razaqpur, G., editors. 'Advanced Composite Materials in Bridges and Structures'. *Proceeding of the Third International Conference*, 2000, Ottawa, Ontario, Canada, 876 p.
8. Biskinis, D.E., Roupakias, G.K. and Fardis, M.N. 'Degradation of Shear Strength of Reinforced Concrete Members with Inelastic Cyclic Displacements', *ACI Structural Journal,* 101 (6), 2004, pp. 773-783.
9. CSA-2006. 'Canadian Highway Bridge Design Code, 2nd Edition, CAN/CSA-S6-00', *Canadian Standard Association*, 2000; Rexdale, Toronto, Ontario, Canada, 734p.
10. El-Ragaby, A., El-Salakawy, E.F., and Benmokrane, B. 'Fatigue Performance of Glass FRP Reinforced Concrete Bridge Deck Slabs', *Proceedings, 2nd fib International Congress,* 2006, Naples, Italy, (proceedings on CD).
11. El-Ragaby, A, El-Salakawy, E.F., and Benmokrane, B. 'Fatigue Life Evaluation of Concrete Bridge Deck Slabs Reinforced with Glass FRP Composite Bars', *ASCE Journal of Composites for Construction,* Vol. 11, No. 3, May/June, 2007, In Print.
12. Kumar, S. and GangaRao, H.V.S. 'Fatigue Response of Concrete Decks Reinforced with FRP Rebars'*, Journal of Structural Engineering, ASCE*, 124 (1): 1998, pp 11-16.
13. Azad, A.K., Baluch, M.H., Al-Mandil, M.Y., Sherif, A.M., and Kareem, K. 'Loss of Punching Capacity of Bridge Deck Slabs from Crack Damage'*, ACI Structural Journal*, 90 (1), 1993, pp. 37-41.
14. Pardikaris, P.C., and Beim, S. 'RC Bridges under Pulsating and Moving Load', *Journal of Structural Engineering, ASCE,* 114 (3), 1988, pp. 591-607.
15. Tanihira, T., Sonoda, K., Horikawa, T., and Kitoh, H. 'Low Cycle Fatigue Characteristics of Bridge Deck RC Slabs under the Repetition of Wheel Loads', *Proceedings, Pacific Concrete Conference,* 1988, New Zealand, pp. 591-607.
16. AASHTO-LRFD. 'Bridge Design Specifications, 2nd edition', *American Association of State Highway and Transportation Officials,* 2002, Washington, DC, USA.
17. El-Ragaby, A., El-Salakawy, E.F., and Benmokrane, B. 'Fatigue Analysis of Concrete Bridge Deck Slabs Reinforced with E-Glass/Vinyl Ester FRP Reinforcing Bars', *Elsevier Journal of Composites, Part B: Engineering*, Vol. 38, Issue 4, June, 2007, pp. 526-534.

CDCC-07

DURABILITY AND FIELD APPLICATIONS OF FIBRE REINFORCED POLYMER (FRP) COMPOSITES FOR CONSTRUCTION

DURABILITÉ ET APPLICATIONS DES COMPOSITES EN POLYMÈRES RENFORCÉS DE FIBRES (PRF) POUR LA CONSTRUCTION

EFFECT OF CFRP SHEETS ON THE CORRODED STEEL - CONCRETE BOND SUBJECTED TO REPEATED LOADING

A. A. Rteil, K. A. Soudki and T. H. Topper

Department of Civil and Environmental Engineering, University of Waterloo, ON, Canada

ABSTRACT

The bond between the steel reinforcement and the concrete is the major factor in preserving the integrity of reinforced concrete (RC) structures. Corrosion of the steel reinforcement is the most common deterioration mechanism for RC structures. It damages the bond between concrete and steel, resulting in an increased deflection and a reduced load carrying capacity of the structures. While several repair materials/methods have been used, fibre reinforced polymer sheets have proved to be better than other alternatives. This paper examines the effect of the corrosion of steel reinforcing bars on the bond between concrete and steel in beams subjected to repeated loading. The repair of these corroded structures with carbon fibre reinforced polymer (CFRP) sheets is also studied. Thirteen bond-beams were tested under repeated loading. The beam dimensions were 152 x 254 x 2000 mm. The variables were the level of corrosion (0% or 5% theoretical mass loss), repair with CFRP sheet and the load range applied. The levels of repeated loading chosen caused a fatigue bond-failure in all the beams. The corrosion decreased the fatigue bond strength on average by 12%. Repairing with CFRP sheets increased the fatigue bond strength by 26% above that of the corroded beams and 11% above that of the uncorroded beams.

1. INTRODUCTION

The corrosion of reinforcing steel is considered to be the main deterioration problem in reinforced concrete structures (RC). The effects of corrosion are two fold: 1) it decreases the area of the steel bar and increases the stress concentration factor, thus decreasing the yield and fatigue capacities of the beam and 2) it induces high tensile stresses in the concrete that lead to longitudinal cracking and in some cases spalling of the concrete cover. These longitudinal cracks decrease the bond capacity between steel and concrete [1]. It is important to maintain the bond between concrete and steel in order to insure a smooth stress transition between the two materials otherwise, an increase in the deflection and a decrease in the load carrying capacity of the RC element results [2].

Structures such as bridges and marine structures are very vulnerable to corrosion and at the same time they are subjected to repeated loading rather than static loading. Repeated loading can cause failure in fatigue even when the applied load is below the static capacity of the RC element [3].

In the last two decades there has been an increase in the use of fibre reinforced polymers (FRP) sheets to repair and strengthen structures because of the various advantages of this new material compared to other traditional repair materials [4]. Recently, the effect of using FRP sheets to repair corroded structures was studied [5]. Results showed that FRP sheets were able to increased the yield load and load carrying capacity for corroded beams compared to corroded unwrapped beams. Also, the confinement provided by the use of FRP sheets increased the bond strength for uncorroded beams [6] as well as corroded beams [7].

However, almost no research has been conducted to check either the effect of corrosion on the bond between steel and concrete under repeated loading regime or the advantages of using FRP sheets to repair such deteriorated RC elements. In order to fill this gap a study was conducted at the University of Waterloo by the authors. This paper presents some of the experimental results obtained so far.

2. EXPERIMENTAL PROGRAM

Thirteen reinforced concrete bond beams were cast and tested. Bond beams were used in this study because they provide more realistic bond behaviour and values compared to other bond specimens such as the pull-out specimens. The bond beam is characterized by un-bonding the concrete and steel in the middle of the beam while keeping them bonded at the ends. This bonded length acts as anchorage length. The dimensions of the beams were 152 mm wide x 254 mm deep x 2000 mm long. Each beam was reinforced with two 20M deformed bars (20 mm in diameter) in tension and with two 8 mm smooth bars in compression. Shear reinforcement was also provided in the form of 8 mm smooth stirrups at a spacing of 125 mm. The bonded length was chosen to be 250 mm. This length, which was smaller than the recommended anchorage length for the steel bars, was chosen so that a bond failure would occur at a load below the steel yield load. Bond failures are characterized by concrete splitting along the bond critical region. To create an un-bonded region in the middle of the specimen a low-density polyethylene tube separated the steel from the concrete. In addition, two pockets at the end of the bonded region allowed easy installation of reinforcing bar instrumentation. These pockets were created by placing high-density foam in the desired locations before casting the beams. A stainless steel hollow tube (9.5 mm in diameter) was provided to be used in the corrosion process. Figure 1 shows the specimen details.

The variables studied were: corrosion level, whether the beams were wrapped with FRP sheets or not and the load range applied on the beam. Table 1 summarizes the test matrix reported in this paper.

In order to achieve the desired corrosion level in a reasonable amount of time the specimens were subjected to accelerated corrosion. The corrosion was initiated by adding

chlorides to the concrete mix, and accelerated by connecting the steel rebars and stainless steel in the specimens to power supplies. The connection was made such that the steel bars acted as anode while the stainless steel acted as a cathode. The specimens were placed in a special environmental chamber to constantly provide the air and water that are also required for the corrosion reactions. The target corrosion level was a 5% mass loss.

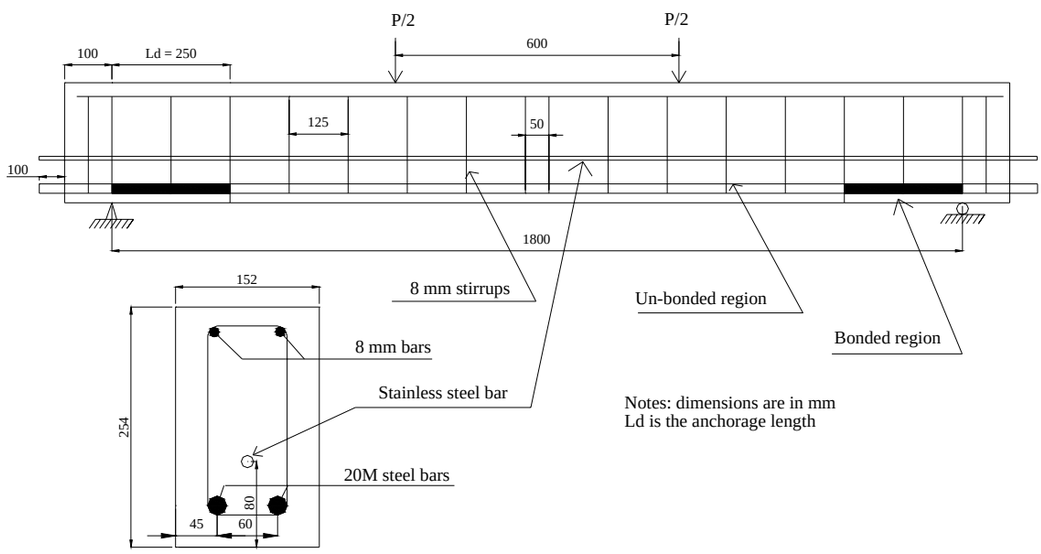

Fig. 1: Longitudinal and cross sectional details for the bond-beam specimen.

Table 1: Test matrix and results

Group	Specimen Notation*	Min. load (kN)	Max load (kN)	Load Range** (%)	FRP	Corrosion Level*** (%)	Fatigue life (N_f)
G1	F45-N-0	10	55	45	No	0	442,134
	F47-N-0	10	57	47			31,423
	F50-N-0	10	60	50			2,041
	F53-N-0	10	63	53			25,052
	F55-N-0	10	65	55			1,714
G2	F37-N-5	10	47	37	No	5	2,912
	F40-N-5	10	50	40			222,263
	F45-N-5	10	55	45			245,318
	F55-N-5	10	65	55			340
G3	F50-W-5	14	83	50	Yes	5	142,208
	F52-W-5	14	85.5	52			523,270
	F55-W-5	14	90	55			17,731
	F65-W-5	14	104	65			113

* Fx-y-z: x is the load range applied as percentage of static load capacity, y = N for un-wrapped specimens and W for wrapped specimens, z is the corrosion level given as theoretical mass loss.
** given as percentage of static load capacity
*** given as theoretical mass loss

One U-shape carbon fibre reinforced polymer (CFRP) sheet, with the fibres oriented normal to the axis of the bars, was used to wrap the specimens of group 3 in their anchorage zones. Prior to the application of the FRP the corrosion cracks were sealed using an epoxy paste adhesive. The cured CFRP sheets properties as supplied by the manufacturer were: tensile strength 715 MPa, tensile modulus 61 GPa, elongation 1.09% and thickness 0.38 mm. The concrete was supplied by a local ready mix plant. It was made with type I cement, and contained no additives. The compressive strength at the time of testing ranged between 40 and 42 MPa. The steel bars used were all grade 400 with nominal yield strength of 440 MPa.

Each specimen was instrumented with 8 linear variable differential transducers (LVDT) to measure the loaded end slip (at the pocket location) and free end slip (at the extended bars). The specimens were tested in four-point bending with a span length of 1800 mm and a constant moment length of 600 mm. The load range applied is given as percentage of the static capacity of the un-corroded specimens. The minimum load was 10% of the static capacity and the maximum load varied depending on the load range chosen. The specimens were tested at a frequency of 1.5 Hz until failure which was defined as the cycle during which the specimen could no longer carry its maximum load.

3. EXPERIMENTAL RESULTS

3.1 General behaviour and mode of failure

While loading the beams for the first time, two flexural cracks opened in the middle of the constant moment zone. Upon cycling the width of those cracks increased, but no more flexural cracks opened because the beam in this area was un-bonded.

For beams in group 1 (un-corroded, un-wrapped), longitudinal cracks opened along the steel bar in the bonded area at both ends of the specimen within the first few cycles. These cracks continued to propagate and increase in number until about 25% of the beams' life. Then they ceased to increase in length, but kept widening at a slow rate until just before failure. At about 90% of the beams' life, the longitudinal cracks in one of the ends of a specimen started to increase rapidly in number and width followed by failure. The failure was brittle, and was accompanied by splitting (and in some cases spalling) in the side and bottom covers along the steel bar (Fig. 2).

The corroded beams in group 2 had longitudinal side and bottom corrosion cracks along the steel bar in the anchored zones before being fatigue tested. In the first 25% to 30% of the beams' life new longitudinal cracks initiated and started to propagate in the anchorage zone and the corrosion cracks widened. Then, the cracks on the surface ceased to lengthen or widen until at about 90% of the beams' life when they started to rapidly increase in length and widen at one end of the beam. This continued until failure. Similar to the un-corroded beams, the failure was sudden and associated by splitting of the concrete cover (Fig. 3).

The CFRP sheets in group 3 did not allow monitoring of surface bond crack initiation and propagation. However, it was noted that the failure of these specimens was associated with CFRP sheets rupturing at one end along the plane of the steel bars at one end of the beam.

After the specimens failed, the CFRP sheets were removed, and the concrete cracks in the end zones were inspected. All the wrapped specimens failed in bond. The failure was associated with longitudinal cracks along the steel bars on one side of the specimen. In general these cracks were finer and less numerous than those in the unwrapped beams (Fig. 4).

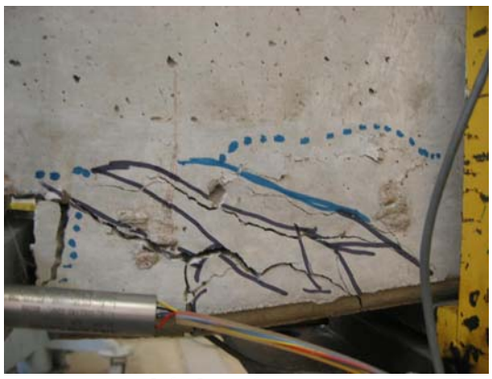

Fig. 2: Typical failure for specimens in G1

Fig. 3: Typical failure for specimens in G2

a) CFRP sheets rupture b) Concrete splitting

Fig. 4: Typical failure for specimens in Group 3

3.2 Fatigue life

The fatigue life results are presented in Table 1 and plotted in Figure 5. In general, the fatigue life increased linearly on a log-log scale as the load range decreased. Corrosion to a 5% theoretical mass loss (group 2) decreased the fatigue bond strength on average by 12% compared to the un-corroded beams (group1). On the other hand, the CFRP sheets increased the fatigue strength of the corroded beams (group 3) by 26% compared to the corroded un-wrapped beams (group 2). Therefore, the CFRP sheets confined the bond critical region and increased the fatigue bond strength of the corroded beams (group 3, dotted lines in Fig. 5) to a level even higher than the control beams by almost 11% (group 1, solid line in Fig. 5).

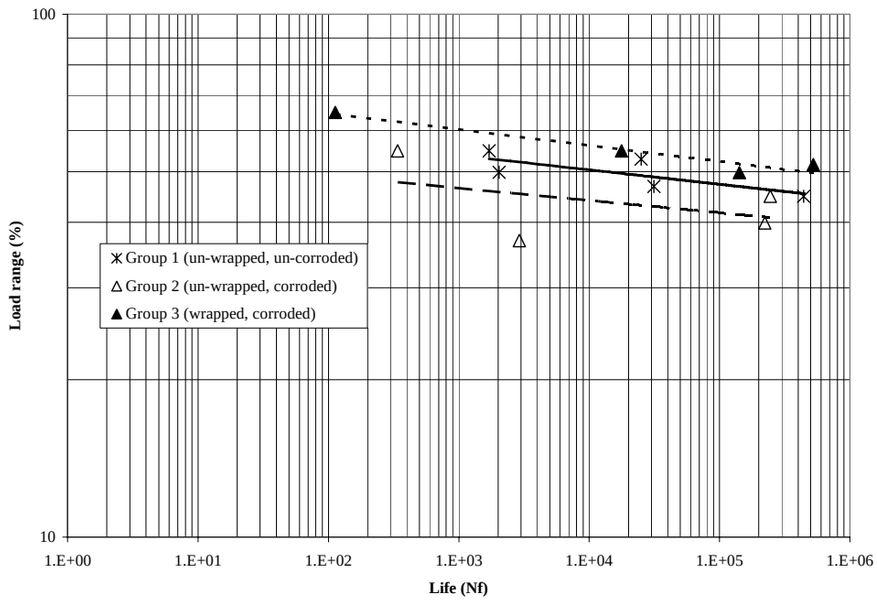

Fig. 5: Load- life variation

3.3 Slip of the steel bars

The typical loaded end slip variation with number of cycles for all the beams presented in this paper is presented in Figure 6. The slip for the unwrapped and uncorroded beams increased in the first 10% of the beams' fatigue life and then stabilized until about 70-80% of the life when it started to increase exponentially until failure (Fig. 6). The slip in the corroded wrapped and unwrapped beams (groups 2 and 3) increased continuously at a constant rate up to 80% to 95% of their life when the slip started to increase exponentially till failure (Fig. 6). Nevertheless, the slip values of the corroded wrapped beams were much higher than those of the uncorroded or the corroded unwrapped beams at any given life percentage.

This difference in behaviour is due to the fact that in the case of the uncorroded beams the sound concrete keys around the steel bar were able to hold the bar from slipping. With continued cycling the bond pressure exerted on these keys caused them to crack. At about 80% of the beams' life these keys were heavily cracked and crushed and the bar slipped at an exponentially increasing rate till failure. On the other hand, the concrete around the steel bars in the unwrapped corroded beams was already cracked due to the tensile pressure exerted by the corrosion products before the tests. Hence, the confinement provided by the concrete to the steel bar for the corroded beams was not as effective as for the uncorroded beams. So, the bar slipped continuously at an almost a constant rate. At about 95% of the beams' life the concrete keys were heavily cracked and crushed and the bar slipped at an exponentially increasing rate until failure as in the case for the uncorroded beams. When the CFRP sheets were added they provided a greater confinement to the concrete around the bar than that provided by concrete alone for either the uncorroded or the corroded beams. Consequently, for a given load range, the wrapped beam attained a much larger slip

displacement and a longer fatigue life (Table 1 and Fig. 7). While the CFRP sheets confined the concrete at the macro scale, the concrete around the bar was cracked by the corrosion stresses and the confinement on the micro scale was lost and the bar slipped continuously throughout the beam's life.

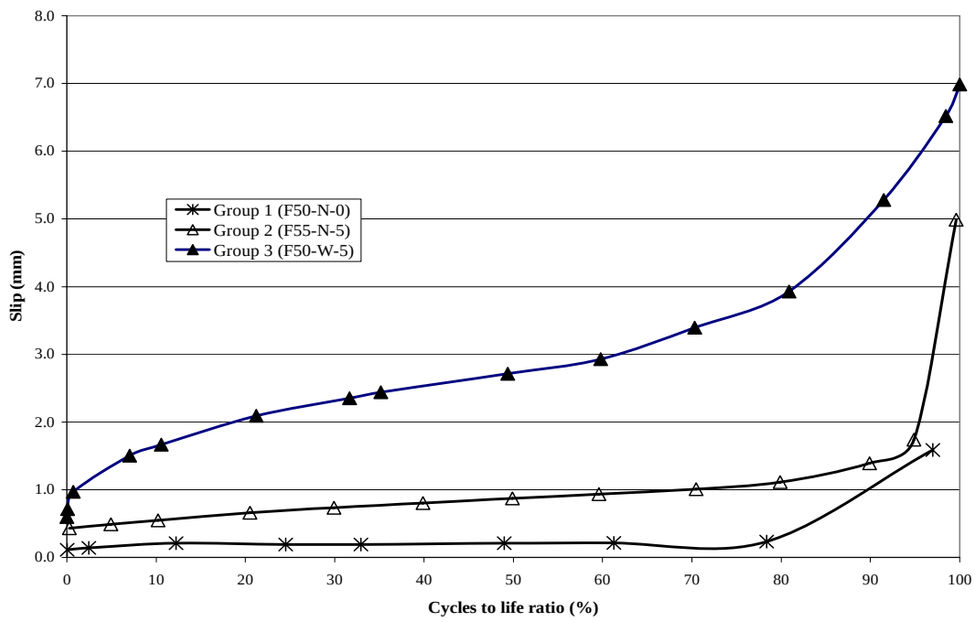

Fig. 6: Typical slip-life variation.

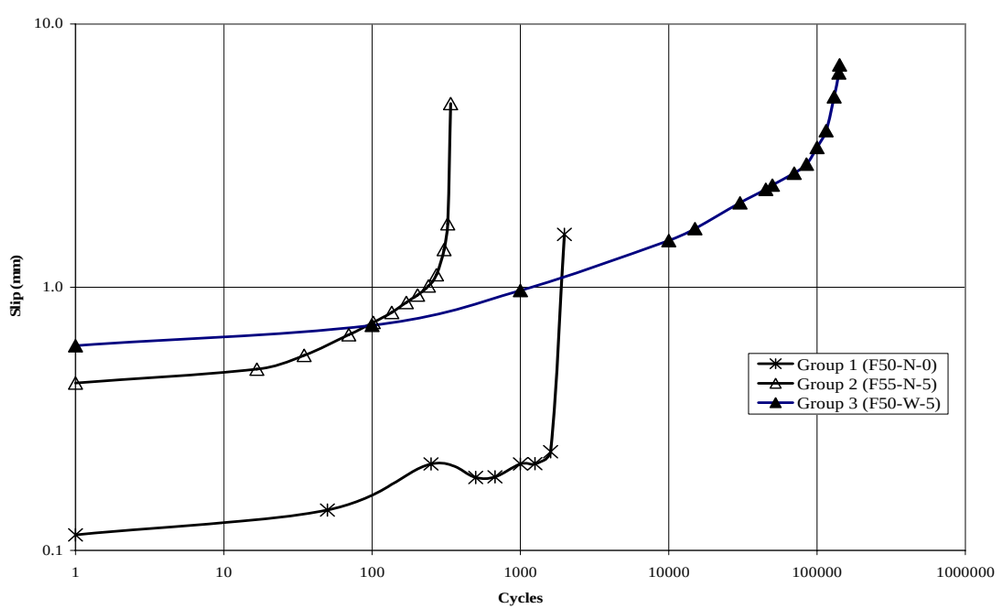

Fig. 7: Typical slip-life variation (log-log scale)

4. CONCLUSIONS

Based on the above discussion the following conclusions can be drawn:

1- Repeated loading caused failure by fatigue of bond for bond-deficient beams.
2- A mild corrosion level (5% theoretical mass loss) caused a 12% reduction in the fatigue bond strength and a change from no slip to a continuous slip increase during most of the fatigue life.
3- CFRP sheets were able to confine the concrete around the corroded steel bars, so that the beams were able to resist higher loads and to attain larger slip values before failure. The fatigue bond strength increased by 26% compared to the corroded unwrapped beams and by 11% compared to the uncorroded unwrapped beams.

5. ACKNOLWLEDGEMENTS

The second author is a project leader in the Network of Centres of Excellence ISIS Canada. The authors would like to thank SIKA Canada for providing the CFRP material. Also, the help of K. Bowman, A. Barber, M. Badawi, S. Ng and R. Al-Hammoud in the lab work is greatly appreciated.

6. REFRENCES

1. ACI Committee 222, 2001, *Corrosion of Metals in Concrete (ACI 222-01)*, Manual of Concrete Practice, American Concrete Institute, Farmington Hills, MI.
2. ACI Committee 408, 1992, *State of the art report on Bond under cyclic loads (ACI 408-92)*, American Concrete Institute, Farmington Hills, MI., USA, 32 pp.
3. ACI Committee 215, 1974, *Considerations for Design of Concrete Structures Subjected to Fatigue Loading (ACI 215-74)*, Manual of Concrete Practice, American Concrete Institute, Farmington Hills, MI.
4. ACI Committee 440, 2002, *Guide for the Design and Construction of Externally Bonded FRP Systems for Strengthening Concrete Structures (ACI 440.2-02)*, American Concrete Institute, Farmington Hills, MI., USA, 45 pp.
5. El Maaddawy, T., Soudki, K., and Topper, T., 2005, 'Long-Term Performance of Corrosion-Damaged Reinforced Concrete Beams', *ACI Structural Journal*, 102 (5), 649-656.
6. Hamad, B.S., Rteil. A.A., Selwan, B. and Soudki, K.A., 2004, "Behaviour of Bond-Critical Regions Wrapped with Fiber-Reinforced Polymer Sheets in Normal and High-Strength Concrete," *ASCE Journal of Composites for Construction*, 8 (3), pp 248-257.
7. Craig, B., and Soudki, K., 2005, 'Post-Repair Performance of Corroded Bond Critical RC Beams Repaired with CFRP', *7th Int'l Symposium on FRP Reinforcement for Concrete Structures, ACI SP-380*, Ed: Shield et al, pp. 563-578.